



# Normal $T_1$ relaxometry and extracellular volume of the pancreas in subjects with no pancreas disease: correlation with age and gender

Temel Tirkes<sup>1</sup> · Jacob R. Mitchell<sup>1</sup> · Liang Li<sup>2</sup> · Xuandong Zhao<sup>3</sup> · Chen Lin<sup>4</sup>

Published online: 28 May 2019  
© Springer Science+Business Media, LLC, part of Springer Nature 2019

## Abstract

**Objective** Determine normal  $T_1$  and extracellular volume (ECV) of the pancreas in subjects with no pancreas disease and correlate with age and gender.

**Subjects and methods** We imaged 120 healthy subjects (age range 20–78 years) who are on annual screening with MRI/MRCP for the possibility of pancreatic cancer. Subjects had a predisposition to develop pancreatic cancer, but no history of pancreas disease or acute symptoms. Equal number ( $n=60$ ) of subjects were scanned on either 1.5 T or 3 T scanner using dual flip angle spoiled gradient echo technique incorporating fat suppression and correction for  $B_1$  field inhomogeneity. Optimization of imaging parameters was performed using a  $T_1$  phantom. ECV was calculated using pre- and post-contrast  $T_1$  of the pancreas and plasma. Regression analysis and Mann–Whitney tests were used for statistical analysis.

**Results** Median  $T_1$  on 1.5 T was 654 ms (IQR 608–700); median  $T_1$  on 3 T was 717 ms (IQR 582–850); median ECV on 1.5 T was 0.28 (IQR 0.21–0.33), and median ECV on 3 T was 0.25 (IQR 0.19–0.28). Age had a mild positive correlation with  $T_1$  ( $r=0.24$ ,  $p=0.009$ ), but not with ECV ( $r=0.06$ ,  $p=0.54$ ).  $T_1$  and ECV were similar in both genders ( $p>0.05$ ).

**Conclusion** This study measured the median  $T_1$  and ECV of the pancreas in subjects with no pancreas disease. Pancreas shows longer  $T_1$  relaxation times in older population, whereas extracellular fraction remains unchanged. Median  $T_1$  values were different between two magnet strengths; however, no difference was seen between genders and ECV fractions.

**Keywords** Pancreas · MRI · Quantitative imaging ·  $T_1$  relaxometry · Extracellular volume

✉ Temel Tirkes  
atirkes@iu.edu  
Jacob R. Mitchell  
jacomitc@iu.edu  
Liang Li  
LLi15@mdanderson.org  
Xuandong Zhao  
zhaoxua@iu.edu  
Chen Lin  
Lin.Chen1@mayo.edu

- <sup>1</sup> Department of Radiology and Imaging Sciences, Indiana University School of Medicine, 550 N. University Blvd. Suite 0663, Indianapolis, IN 46202, USA
- <sup>2</sup> Department of Biostatistics, The University of Texas MD Anderson Cancer Center, 1400 Pressler Street, Unit 1411, FCT4.6008, Houston, TX 77030, USA
- <sup>3</sup> Department of Radiology and Imaging Sciences, Indiana University School of Medicine, R2 E124G, 950 W Walnut Street, Indianapolis, IN 46202, USA
- <sup>4</sup> Department of Radiology, Mayo Clinic, 4500 San Pablo Rd, Jacksonville, FL 32224, USA

## Abbreviations

ECV Extracellular volume  
MRCP Magnetic resonance cholangiopancreatography  
MRI Magnetic resonance imaging  
3D Three-dimensional

## Introduction

Quantitative MRI is becoming increasingly common in current radiology research and practice, assisting in the clinical assessment of many patients with a spectrum of diseases [1]. Novel quantitative MR imaging techniques provide in vivo characterization of tissues and have potential to be a non-invasive biomarker to diagnose certain solid organ pathologies. Quantitative imaging metrics can also be used to monitor the course of therapy in clinical trials [2].  $T_1$  relaxometry measures the specific  $T_1$  relaxation time of a tissue. A number of quantitative MRI studies have been published reporting the alterations of  $T_1$  in a variety of pathologic conditions in the abdomen [3–5]. These studies focused on

detecting tissue fibrosis; seen with cirrhosis [6–8], chronic pancreatitis [9], and kidney failure [10].  $T_1$  measured during pre- and post-contrast phase are used to calculate the extracellular volume (ECV). ECV imaging calculates the extracellular fraction of a solid organ, which is known to increase as a result of adverse tissue remodeling leading to tissue fibrosis [4, 5]. It has been shown to be useful for evaluation of myocardial fibrosis [11, 12], cirrhosis [4, 8], and chronic pancreatitis [5]. However, there are insufficient data on normal quantitative metrics of the pancreas and correlation with biometric parameters (e.g., age and sex). More investigations are needed to determine the normal values and reach a consensus on the amount of change that should be considered clinically significant pathology. The purpose of this study was to determine normal  $T_1$  and ECV of the pancreas in subjects with no pancreas disease and correlate these quantitative metrics with age and gender.

## Subjects and methods

### Subjects

This study was compliant with the Health Insurance Portability and Accountability Act and waiver of informed consent was obtained from the Institutional Review Board. We prospectively imaged 120 non-consecutive subjects between June 2016 and December 2018. The subjects were enrolled in the pancreatic cancer screening program and were being screened annually for pancreatic cancer with magnetic resonance cholangiopancreatography (MRCP). The purpose of this screening program is to do surveillance on subjects with a family history of pancreatic cancer or was found to have a genetic predisposition (e.g., positive BRCA) to develop pancreatic cancer, but otherwise were healthy individuals. All subjects were screened with serum amylase, lipase, AST, alkaline phosphatase, CEA, CA19-9, and c-peptide levels before enrolling into the program. MRCP images of all the subjects were reviewed by a single radiologist and only those with Cambridge grade 0 (normal) [13] were included in the study. Subjects who did not receive intravenous contrast ( $n = 17$ ), diagnosed with cystic pancreatic neoplasm ( $n = 11$ ), or with pancreatic adenocarcinoma ( $n = 1$ ) were also excluded from the study.

### $T_1$ imaging

$T_1$  maps were acquired at pre-contrast and 6-min late enhancement phases using a dual flip angle three-dimensional (3D) spoiled gradient echo technique (Fig. 1). Subjects were imaged on either 1.5 T (Magnetom Avanto Fit, Siemens Medical Solutions, Malvern, PA) or 3 T scanner (Magnetom Verio, Siemens Medical Solutions, Malvern,

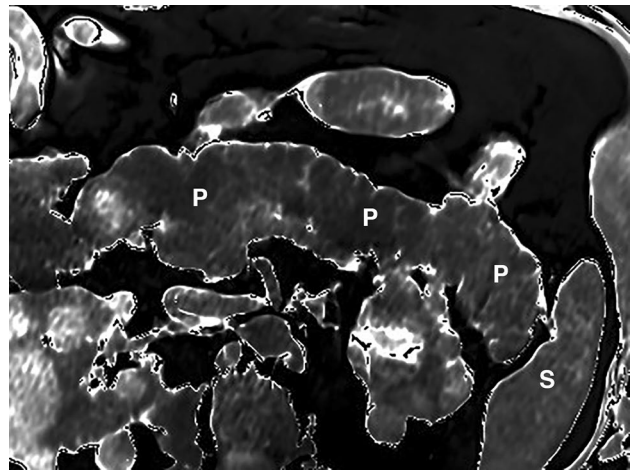


**Fig. 1** This is an axial  $T_1$  map in a 51-year-old man with family history of pancreatic cancer on surveillance.  $T_1$  maps can be depicted either as a grayscale or colormap. Region of interest measurements obtained from the grayscale image reveals the  $T_1$  relaxation time (P pancreas, S spleen)

PA) using a commercially available  $T_1$  mapping pulse sequence (MapIt, Siemens Medical Solutions, Malvern, PA). Fat suppression was not utilized. Vendor supplied correction for  $B_1$  field inhomogeneity was employed. The imaging parameters were: 48 axial slices of 4 mm thickness, field of view of 360, acquisition matrix of  $320 \times 168$ , and parallel imaging factor of 2 (Siemens GRAPPA). The 1.5 T scanner used TR of 7.4 ms, TE of 2.39 ms, and flip angles of  $3^\circ$  and  $19^\circ$ , while the 3 T scanner used TR of 3.87 ms, TE of 1.32 ms, and flip angles of  $2^\circ$  and  $13^\circ$ . Acquisition time was approximately 20 s (1 breath-hold).  $T_1$  maps were reconstructed on the MR scanner using vendor supplied software. To ensure accurate measurements of the  $T_1$ , phantom testing was performed using a commercially available unit (System phantom model 130, High Precision Device, Inc.). This phantom includes an array of elements of which  $T_1$  values were verified by the National Institute of Standards and Technology (NIST). The phantom tests showed excellent precision for both 1.5 T ( $\rho_c = 0.9962$ ) and 3 T scanners ( $\rho_c = 0.9974$ ).

### ECV imaging

Gadobenate dimeglumine (MultiHance, Bracco Diagnostics Inc., Monroe Township, NJ) was administered in all subjects using the manufacturer recommended dose of 0.1 mmol/kg.  $T_1$  relaxation time was measured by a single radiologist in pre and post-contrast phases, using average of the region of interest values obtained from the head, body, and tail of the pancreas. Attention was given to obtain the signal from the homogenous part of the gland, excluding the duct and vessels. The approximate diameter of the circle region of

interest was 15 mm. Blood pool signal was obtained from the aortic lumen to find out the plasma  $T_1$  relaxivity. The aortic lumen signal is prone to inflow artifact and therefore,  $T_1$  was measured from the aortic lumen by taking the average ROI value of 5 consecutive image slices below the level of pancreas. These values were entered into this formula to calculate ECV fraction:

$$ECV = \frac{(1 - \text{hematocrit}) \times \Delta R1_{\text{target}}}{\Delta R1_{\text{blood}}}$$

where  $\Delta R1_{\text{target}}$  and  $\Delta R1_{\text{blood}}$  are defined as the change of  $1/T_1$  relaxation rate in pancreas and blood pool relaxivity before and after contrast administration.  $T_1$  is a time constant describing the longitudinal relaxation rate, and its reciprocal ( $1/T_1$ ) is referred to as  $R_1$ . The change in  $R_1$  ( $\Delta R_1$ ) is defined as:  $\Delta R_1 = (R_1 \text{ post-contrast}) - (R_1 \text{ pre-contrast})$ .  $\Delta R_1$  is proportional to Gadolinium (Gd) concentration when both tissues are in equilibrium;  $\Delta R1_{\text{pancreas}}/\Delta R1_{\text{blood}} = [\text{Gd}]_{\text{pancreas}}/[\text{Gd}]_{\text{blood}}$ . Since the gadolinium chelates, such as Gd-BOPTA are extracellular agents, the ratio of contrast agent concentrations between pancreas and blood equals the ratio of extracellular volume between the tissues:  $[\text{Gd}]_{\text{pancreas}}/[\text{Gd}]_{\text{blood}} = ECV_{\text{pancreas}}/ECV_{\text{blood}}$ . The ECV of the blood is defined as the fraction of the blood volume which is not composed of blood cells, in other words, the fraction composed of plasma. The plasma volume was easily calculated as:  $ECV_{\text{blood}} = [1 - \text{hematocrit}]$ . ECV maps were generated offline, using a prototype software (MR Arithmetics; Siemens Healthcare) (Fig. 2). Non-rigid registration was also performed using this software between the pre- and post-contrast  $T_1$  maps to eliminate misregistration due to differences in breath-hold.

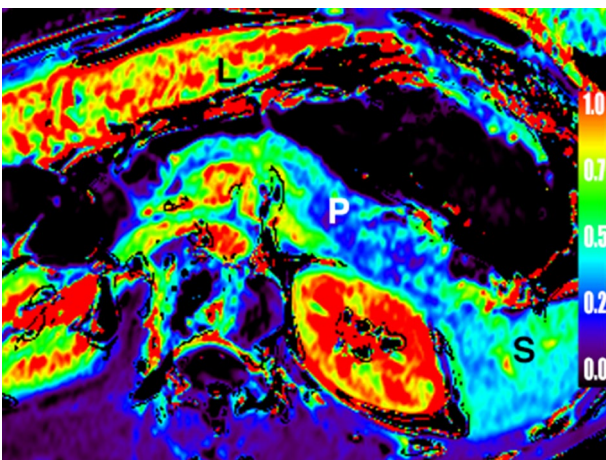


**Fig. 2** ECV map of the pancreas. This is a 37-year-old woman with BRCA 2 gene mutation on surveillance for pancreatic cancer. An axial color scale ECV map is shown. (P pancreas, S spleen, L liver)

## MRCP imaging

Secretin enhanced MRCP was performed following intravenous administration of 16  $\mu\text{g}$  of secretin (ChiRhoStim, ChiRhoClin Inc., Burtonsville, MD) via slow infusion over one minute. Immediately following injection, the pancreas was imaged using a coronal 2D single-shot turbo spin echo sequence (HASTE, Siemens Medical Solutions, Malvern, PA), which is repeated every 20 s up to 8 min. No adverse events were encountered.

## Statistical analysis

Regression analysis was used to evaluate the correlation of the  $T_1$  and ECV with the age. Correlation coefficients were interpreted as: mild, 0.2; moderate, 0.5; strong, 0.8; and perfect, 1.0 [14]. Mann–Whitney test was used to determine the median and interquartile range (IQR) at different age groups for the  $T_1$  and ECV, also for assessing the differences between the gender, 1.5 T and 3 T magnet strengths. If the resulting  $p$  value is  $< 0.05$ , a statistically significant difference between the two samples was accepted. The precision of the  $T_1$  imaging technique was evaluated using the concordance correlation coefficient. The concordance correlation coefficient quantifies the agreement between two measures such that when they are plotted against each other, higher concordance correlation coefficient corresponds to a lesser deviation from the 45-degree line. The scale of concordance correlation coefficient ( $\rho_c$ ) is considered as poor  $< 0.90$ ; moderate 0.90–0.95; substantial 0.95–0.99; and almost perfect  $> 0.99$  [15]. Statistical analyses were performed using MedCalc version 18.11.3 (MedCalc Software, Mariakerke, Belgium).

## Results

Subjects were between 20 and 78 years of age (mean: 48). There were 32 males and 88 females. Table 1 shows that there was no difference between two genders in terms of age of subjects scanned at 1.5 T ( $p = 0.77$ ) and 3 T ( $p = 0.84$ ); ECV at 1.5 T ( $p = 0.09$ ) and 3 T ( $p = 0.55$ ); and  $T_1$  at 1.5 T ( $p = 0.47$ ) and 3 T ( $p = 0.09$ ). Therefore, results from both genders were combined in the analysis.

Table 2 lists  $T_1$  measured at 1.5 T and 3 T scanners. Median  $T_1$  at 1.5 T was 654 ms (IQR 608–700) and was statistically different than  $T_1$  of 717 ms (IQR 582–850) measured at 3 T ( $p = 0.03$ ). Table 3 lists the median ECV calculated at 1.5 T and 3 T scanners. Median ECV at 1.5 T was 0.28 (IQR 0.21–0.33) and was similar to ECV of 0.25 (IQR 0.19–0.28) at 3 T ( $p = 0.06$ ).

**Table 1** Effect of gender and MR field strength on  $T_1$  relaxation time (ms) and ECV of the pancreas

	Male <i>n</i> = 32		Female <i>n</i> = 88		<i>p</i> value
	Median	IQR	Median	IQR	
$T_1$ (ms)					
1.5 T	659	[571–707]	649	[609–696]	0.47
3.0 T	636	[551–712]	753	[637–871]	0.09
ECV (fraction)					
1.5 T	0.25	[0.17–0.32]	0.29	[0.24–0.34]	0.09
3.0 T	0.24	[0.20–0.26]	0.25	[0.19–0.29]	0.55
Age (years)					
1.5 T	48	[37–59]	48	[37–58]	0.77
3.0 T	52	[43–58]	52	[43–59]	0.84

There was no statistically significant difference between two genders in terms of  $T_1$ , ECV, and age

ECV extracellular volume fraction, IQR interquartile range

**Table 2**  $T_1$  relaxation time of the pancreas at 1.5 T and 3 T magnet field strength separated by age groups

Age groups	1.5 T		3 T	
	$T_1$	<i>n</i>	$T_1$	<i>n</i>
All ages	654 ms [608–700]	60	717 ms [582–850]	60
Age 20–29	678 ms [575–763]	9	642 ms [533–712]	5
Age 30–39	645 ms [609–735]	12	653 ms [428–772]	11
Age 40–49	655 ms [637–697]	12	734 ms [600–859]	11
Age 50–59	608 ms [557–690]	15	753 ms [640–885]	19
Age 60–69	671 ms [628–697]	10	762 ms [576–965]	10
Age 70–79	645 ms [610–680]	2	807 ms [714–984]	4

There was a significant difference in  $T_1$  between the 1.5 and 3 T when all age groups were combined ( $p=0.03$ )

Numbers in bracket indicate interquartile range (IQR)

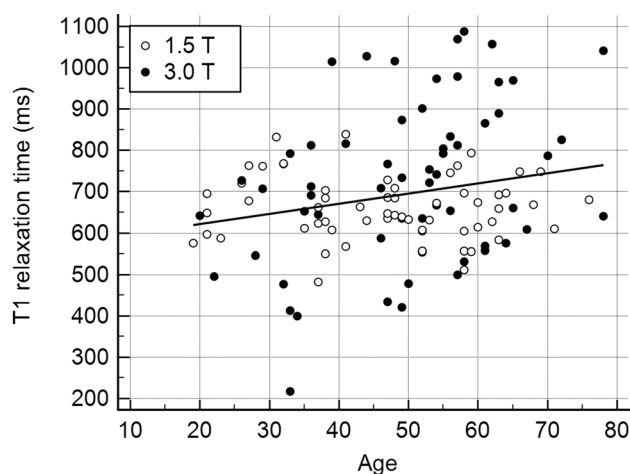
**Table 3** ECV of the pancreas at 1.5 and 3 T scanners separated by age groups

Age Groups	1.5 T		3 T	
	ECV fraction	<i>n</i>	ECV fraction	<i>n</i>
All Ages	0.28 [0.21–0.33]	60	0.24 [0.19–0.28]	60
Age 20–29	0.34 [0.30–0.39]	9	0.25 [0.22–0.26]	5
Age 30–39	0.25 [0.19–0.29]	12	0.19 [0.14–0.23]	11
Age 40–49	0.25 [0.20–0.33]	12	0.24 [0.19–0.33]	11
Age 50–59	0.31 [0.22–0.36]	15	0.26 [0.22–0.27]	19
Age 60–69	0.27 [0.22–0.28]	10	0.27 [0.22–0.32]	10
Age 70–79	0.23 [0.23–0.23]	2	0.27 [0.23–0.34]	4

There was no significant difference in median ECV between the two magnet strengths when all age groups were combined ( $p=0.06$ )

ECV Extracellular volume fraction

Numbers in bracket indicate interquartile range (IQR)

**Fig. 3** Effect of age on  $T_1$  properties of the pancreas. There is a mild positive correlation between  $T_1$  relaxation time and age ( $r=0.24$ ,  $p=0.009$ )

$T_1$  relaxation time had a mild positive correlation with age ( $r=0.24$ ,  $p=0.009$ ) (Fig. 3). ECV did not have a correlation with age ( $r=0.06$ ,  $p=0.54$ ).

## Discussion

$T_1$  relaxometry and ECV may provide useful applications in the abdominal imaging however more investigations are needed to explore the full potential. The primary objective of this study was to determine the normal  $T_1$  and ECV of the pancreas in subjects with no pancreas disease. We expect that this information can be used as a reference in future studies. Secondary objectives were to determine whether  $T_1$  and ECV change with age, gender, or MR signal strength. To our knowledge, none of this information was previously reported in the radiology literature.

Our first observation was that the median  $T_1$  of the pancreas were different between 1.5 T and 3 T scanners when all age groups were combined. It is well known that the longitudinal relaxation time ( $T_1$ ) is longer at higher magnetic field than at lower magnetic field [16, 17] therefore different threshold values should be used for different magnet strengths. As the main  $B_0$  field strength increases, the resonance frequency of the excited spins also increases (from approximately 64 MHz at 1.5 T to 128 MHz at 3 T) [18]. The higher frequency of the spins reduces the efficiency of energy transfer, resulting in longer  $T_1$  relaxation times at 3 T [19]. We found the ECV fractions at 1.5 and 3 T to be similar.

Our second significant finding was that age had a mild positive correlation with  $T_1$ . Many studies reported correlation of  $T_1$  signal intensity of the pancreas with fibrosis

(determined by histopathology), bicarbonate level measured via endoscopic pancreatic function tests, or evidence of chronic pancreatitis determined by Cambridge classification [20–23]. This is the first study showing that pancreas is slowly losing its shorter  $T_1$  relaxation property over the period of decades. On the other hand, ECV remained the same over a wide range of subjects age (20–78 years), indicating that extracellular to intracellular ratio is not altered in subjects with no pancreas disease.

Our third finding was that, both genders had similar ECV fraction and  $T_1$ . Therefore, we combined both genders in the analysis.

We used a commercially available  $T_1$  mapping pulse sequence which utilizes 3D dual flip angle spoiled gradient echo technique to acquire  $T_1$  maps of the entire upper abdomen in one breath-hold. Currently, there is no consensus about which  $T_1$  mapping pulse sequence is ideal for abdominal imaging. Conventional Look-Locker  $T_1$  mapping sequences require long imaging times [24] and will be challenging for abdominal imaging which large spatial coverage is essential. Efforts have been made to modify the Look-Locker method [25] by combining it with a stack-of-spirals acquisition accelerated using 3D through-time spiral GRAPPA reconstruction; producing 32 images per breath-hold. These new methods require more studies for validation and support from vendors. Recently, a novel approach named MR fingerprinting was introduced [26]. Instead of using a repeated, serial acquisition of data for the characterization of individual parameters of interest, MR fingerprinting uses a pseudorandomized acquisition that causes the signals from different tissues to have a unique signal evolution or ‘fingerprint’ that is simultaneously a function of the multiple material properties. The processing after acquisition involves a pattern recognition algorithm to match the fingerprints to a predefined dictionary of predicted signal evolutions. A recent MR fingerprinting study on 14 asymptomatic subjects reported  $T_1$  of the liver, kidney, spleen, skeletal muscle, and fat [27] but did not report  $T_1$  of the pancreas.

ECV imaging can distinguish intra- and extracellular spaces of the tissues and calculates the fraction of the extracellular volume. ECV imaging is based on the concept that extracellular matrix increases when tissues are subjected to repetitive inflammation leading tissue remodeling and eventually fibrosis. MRI is an ideal modality to calculate ECV since the gadolinium diffuses from the intravascular to the extracellular space of the tissues. ECV is calculated by measuring the  $T_1$  of the plasma and the target tissue before and after contrast injection. We used the aortic lumen to determine the blood plasma relaxivity since it has a larger diameter than other vessels and has been successfully used in prior studies [5, 28]. It should be noted that the dual flip angle sequence is susceptible to pulsatile flow in the aorta. Other pulse sequences with cardiac gating produce more

stable aortic signal; however, the downside is acquisition of only 1–3 images per breath-hold.

One of the limitations of this study was that the population of 120 subjects became small when divided by 6 age groups, especially in the age 70–78 group. The subjects were predominantly females; however, results showed that gender difference did not effect  $T_1$  and ECV. Our study included subjects with a genetic predisposition for pancreatic cancer, however, had no known pancreatic disease or symptoms at the time of the study. We further screened the subjects with secretin enhanced MRCP and included only those with Cambridge grade 0. Nevertheless, when determining the normal quantitative MR metrics, it would be ideal to image healthy volunteers at multiple institutions by comparing different MR vendors and imaging techniques.

In conclusion, this study measured the median  $T_1$  and ECV of the pancreas in subjects with no pancreas disease. Pancreas shows longer  $T_1$  relaxation times in older population, whereas extracellular fraction remains unchanged. No difference was seen between genders. Separate  $T_1$  values should be used for 1.5 and 3 T scanners.

**Funding** Dr. Tirkes is supported by National Cancer Institute and National Institute of Diabetes and Digestive and Kidney Diseases of the National Institutes of Health under award numbers 1R01DK116963 and U01DK108323 (Consortium for the Study of Chronic Pancreatitis, Diabetes, and Pancreatic Cancer). The content is solely the responsibility of the authors and does not necessarily represent the official views of the National Institutes of Health. Dr. Li is supported by National Cancer Institute and National Institute of Diabetes and Digestive and Kidney Diseases of the National Institutes of Health under award numbers U01DK108323 and 1R01DK116963. Dr. Li also receives support from MD Anderson Cancer Center under grant number P30CA016672.

## Compliance with ethical standards

**Informed consent** This study was approved by the Institutional Review Board and the requirement for informed consent was waived.

## References

1. Rosenkrantz AB, Mendiratta-Lala M, Bartholmai BJ, Ganeshan D, Abramson RG, Burton KR, Yu JP, Scalzetti EM, Yankeeol TE, Subramaniam RM, Lenchik L (2015) Clinical utility of quantitative imaging. *Acad Radiol* 22 (1):33–49. <https://doi.org/10.1016/j.acra.2014.08.011>
2. Messroghli DR, Greiser A, Frohlich M, Dietz R, Schulz-Menger J (2007) Optimization and validation of a fully-integrated pulse sequence for modified look-locker inversion-recovery (MOLLI) T1 mapping of the heart. *J Magn Reson Imaging* 26 (4):1081–1086. <https://doi.org/10.1002/jmri.21119>
3. Moon JC, Messroghli DR, Kellman P, Piechnik SK, Robson MD, Ugander M, Gatehouse PD, Arai AE, Friedrich MG, Neubauer S, Schulz-Menger J, Schelbert EB, Society for Cardiovascular Magnetic Resonance I, Cardiovascular Magnetic Resonance Working Group of the European Society of C (2013) Myocardial

- T1 mapping and extracellular volume quantification: a Society for Cardiovascular Magnetic Resonance (SCMR) and CMR Working Group of the European Society of Cardiology consensus statement. *J Cardiovasc Magn Reson* 15:92. <https://doi.org/10.1186/1532-429x-15-92>
4. Ou HY, Bonekamp S, Bonekamp D, Corona-Villalobos CP, Torbenson MS, Geiger B, Kamel IR (2013) MRI arterial enhancement fraction in hepatic fibrosis and cirrhosis. *AJR Am J Roentgenol* 201 (4):W596-602. <https://doi.org/10.2214/ajr.12.10048>
  5. Tirkes T, Lin C, Cui E, Deng Y, Territo PR, Sandrasegaran K, Akisik F (2018) Quantitative MR Evaluation of Chronic Pancreatitis: Extracellular Volume Fraction and MR Relaxometry. *AJR Am J Roentgenol* 210 (3):533-542. <https://doi.org/10.2214/ajr.17.18606>
  6. Kim KA, Park MS, Kim IS, Kiefer B, Chung WS, Kim MJ, Kim KW (2012) Quantitative evaluation of liver cirrhosis using T1 relaxation time with 3 tesla MRI before and after oxygen inhalation. *J Magn Reson Imaging* 36 (2):405-410. <https://doi.org/10.1002/jmri.23620>
  7. Curtis WA, Fraum TJ, An H, Chen Y, Shetty AS, Fowler KJ (2019) Quantitative MRI of Diffuse Liver Disease: Current Applications and Future Directions. *Radiology* 290 (1):23-30. <https://doi.org/10.1148/radiol.2018172765>
  8. Luetkens JA, Klein S, Traber F, Schmeel FC, Sprinkart AM, Kuetting DLR, Block W, Uschner FE, Schierwagen R, Hittatiya K, Kristiansen G, Gieseke J, Schild HH, Trebicka J, Kukuk GM (2018) Quantification of Liver Fibrosis at T1 and T2 Mapping with Extracellular Volume Fraction MRI: Preclinical Results. *Radiology* 288 (3):748-754. <https://doi.org/10.1148/radiol.2018180051>
  9. Tirkes T, Lin C, Fogel EL, Sherman SS, Wang Q, Sandrasegaran K (2017) T1 mapping for diagnosis of mild chronic pancreatitis. *J Magn Reson Imaging* 45 (4):1171-1176. <https://doi.org/10.1002/jmri.25428>
  10. Huang Y, Sadowski EA, Artz NS, Seo S, Djamali A, Grist TM, Fain SB (2011) Measurement and comparison of T1 relaxation times in native and transplanted kidney cortex and medulla. *J Magn Reson Imaging* 33 (5):1241-1247. <https://doi.org/10.1002/jmri.22543>
  11. Kellman P, Wilson JR, Xue H, Bandettini WP, Shanbhag SM, Druey KM, Ugander M, Arai AE (2012) Extracellular volume fraction mapping in the myocardium, part 2: initial clinical experience. *J Cardiovasc Magn Reson* 14:64. <https://doi.org/10.1186/1532-429x-14-64>
  12. Ugander M, Oki AJ, Hsu LY, Kellman P, Greiser A, Aletras AH, Sibley CT, Chen MY, Bandettini WP, Arai AE (2012) Extracellular volume imaging by magnetic resonance imaging provides insights into overt and sub-clinical myocardial pathology. *Eur Heart J* 33 (10):1268-1278. <https://doi.org/10.1093/eurheartj/ehr481>
  13. Axon AT, Classen M, Cotton PB, Cremer M, Freeny PC, Lees WR (1984) Pancreatography in chronic pancreatitis: international definitions. *Gut* 25 (10):1107-1112
  14. Zou KH, Tuncali K, Silverman SG (2003) Correlation and simple linear regression. *Radiology* 227 (3):617-622. <https://doi.org/10.1148/radiol.2273011499>
  15. Lin LI (1989) A concordance correlation coefficient to evaluate reproducibility. *Biometrics* 45 (1):255-268
  16. de Bazelaire CM, Duhamel GD, Rofsky NM, Alsop DC (2004) MR imaging relaxation times of abdominal and pelvic tissues measured in vivo at 3.0 T: preliminary results. *Radiology* 230 (3):652-659. <https://doi.org/10.1148/radiol.2303021331>
  17. Rinck PA, Muller RN (1999) Field strength and dose dependence of contrast enhancement by gadolinium-based MR contrast agents. *Eur Radiol* 9 (5):998-1004. <https://doi.org/10.1007/s003300050781>
  18. Soher BJ, Dale BM, Merkle EM (2007) A review of MR physics: 3T versus 1.5T. *Magn Reson Imaging Clin N Am* 15 (3):277-290, v. <https://doi.org/10.1016/j.mric.2007.06.002>
  19. Stanisz GJ, Odobina EE, Pun J, Escaravage M, Graham SJ, Bronskill MJ, Henkelman RM (2005) T1, T2 relaxation and magnetization transfer in tissue at 3T. *Magn Reson Med* 54 (3):507-512. <https://doi.org/10.1002/mrm.20605>
  20. Winston CB, Mitchell DG, Outwater EK, Ehrlich SM (1995) Pancreatic signal intensity on T1-weighted fat saturation MR images: clinical correlation. *J Magn Reson Imaging* 5 (3):267-271
  21. Balci NC, Smith A, Momtahan AJ, Alkaade S, Fattahi R, Tariq S, Burton F (2010) MRI and S-MRCP findings in patients with suspected chronic pancreatitis: correlation with endoscopic pancreatic function testing (ePFT). *J Magn Reson Imaging* 31 (3):601-606. <https://doi.org/10.1002/jmri.22085>
  22. Tirkes T, Fogel EL, Sherman S, Lin C, Swensson J, Akisik F, Sandrasegaran K (2017) Detection of exocrine dysfunction by MRI in patients with early chronic pancreatitis. *Abdom Radiol (NY)* 42 (2):544-551. <https://doi.org/10.1007/s00261-016-0917-2>
  23. Watanabe H, Kanematsu M, Tanaka K, Osada S, Tomita H, Hara A, Goshima S, Kondo H, Kawada H, Noda Y, Tanahashi Y, Kawai N, Yoshida K, Moriyama N (2014) Fibrosis and postoperative fistula of the pancreas: correlation with MR imaging findings—preliminary results. *Radiology* 270 (3):791-799. <https://doi.org/10.1148/radiol.13131194>
  24. Kimelman T, Vu A, Storey P, McKenzie C, Burstein D, Prasad P (2006) Three-dimensional T1 mapping for dGEMRIC at 3.0 T using the Look Locker method. *Invest Radiol* 41 (2):198-203
  25. Chen Y, Lee GR, Aandal G, Badve C, Wright KL, Griswold MA, Seiberlich N, Gulani V (2016) Rapid volumetric T1 mapping of the abdomen using three-dimensional through-time spiral GRAPPA. *Magn Reson Med* 75 (4):1457-1465. <https://doi.org/10.1002/mrm.25693>
  26. Ma D, Gulani V, Seiberlich N, Liu K, Sunshine JL, Duerk JL, Griswold MA (2013) Magnetic resonance fingerprinting. *Nature* 495 (7440):187-192. <https://doi.org/10.1038/nature11971>
  27. Chen Y, Jiang Y, Pahwa S, Ma D, Lu L, Twieg MD, Wright KL, Seiberlich N, Griswold MA, Gulani V (2016) MR Fingerprinting for Rapid Quantitative Abdominal Imaging. *Radiology* 279 (1):278-286. <https://doi.org/10.1148/radiol.2016152037>
  28. Bandula S, Banypersad SM, Sado D, Flett AS, Punwani S, Taylor SA, Hawkins PN, Moon JC (2013) Measurement of Tissue interstitial volume in healthy patients and those with amyloidosis with equilibrium contrast-enhanced MR imaging. *Radiology* 268 (3):858-864. <https://doi.org/10.1148/radiol.13121889>

**Publisher's Note** Springer Nature remains neutral with regard to jurisdictional claims in published maps and institutional affiliations.